Finite Element Analysis of the Longitudinal Impact of a Rod with Various Support Conditions

Ragab M. Etiwa, Hanaa M. Elabsy, and Hesham A. Elkaranshawy
Department of Engineering Mathematics and Physics, Alexandria University, Engineering Mechanics Division, Alexandria, Egypt
Email: ragab.etiwa@alexu.edu.eg, h.elabsy@hotmail.com, hesham_elk@alexu.edu.eg

***Abstract*— In this paper, a finite element formulation is developed to analyze the stress wave propagation in an elastic rod struck by a rigid body. The rod has either rigid, free, or deformable support conditions. The formulation is based upon Saint-Venant's contact theory. Accordingly, the equations of motion are introduced, and the equivalent finite element formulation is obtained. Hence, the dynamic responses are illustrated, and contact forces are evaluated. Certain simulation results are compared to the corresponding published analytical results. Results demonstrate the influence of the support condition on the propagated stress wave and consequently on the velocities, the displacements, and the contact forces. A simulated visualization for the reflection and transmission of the stress wave at the constraint end is presented to improve the perception of the phenomenon.**

***Index Terms*—wave propagation, longitudinal impact, newmark integration method, finite element method, longitudinal vibration**

I. INTRODUCTION

In many engineering applications, impacts of elastic bodies are a common problem, resulting from collisions of moving bodies. Investigation of impact has been extensively studied for a long time [1]–[7]. The most famous device that utilizes a longitudinal impact to generate stress waves is known as the Hopkinson's bar [6], [8]. Hopkinson's bar has been used for different applications such as testing and driving of pile and soil testing in geotechnical engineering, percussive drilling in terrestrial mining, and drilling devices in the aerospace application to explore the subsurface of Lunar, Martian [9], [10]. Along with other applications of the Hopkinson bar are the determination of some dynamic strength of materials at high strain rate [11]–[13] as well as calibration of shock accelerometers [14], [15].

The generation of a longitudinal stress wave in elastic rods by the impact of a rigid body was treated by Saint-Venant and Boussinesq [4] using the theory of wave propagation. The assumptions of the analysis include propagation of stress waves in one-dimension, perfectly plane contact surfaces, and neglecting the wave propagation and deformation of the striking body.
The wave theory is reviewed by Goldsmith [1], Graf [2], Timoshenko [3], Love [4], and Johnson [5]. Increasing in times of wave traveling along the rod, the method leads to complicated wave equations, and this made it difficult to be used.

The numerical methods have been used in the study of longitudinal impacts of rod structures, Elkaranshawy [16]–[18] and Ragab [19] investigated this problem using the finite element method, also the dynamic substructure method has been used in the analysis of impacts in uniform and non-uniform rod structures by Shen [20], [21]. Zhu and Xing [22] used the direct mode superposition method to obtain the analytical solution of impact problems.

In this paper, based on Saint-Venant's wave theory and using the finite element method (FEM), the dynamic response and the stress wave propagation of the longitudinal impact of a rigid mass on a bar with rigid, free, and elastic support conditions are fully analyzed. The finite element results are compared with the analytical results of the wave theory to verify the validation of using the finite element in the analysis of impacts of rod structures.

II. MATHEMATICAL MODELING

Considering a stationary homogenous elastic rod with mass m, young modulus E, density ρ, uniform cross-section area A, and length L and is struck on the right end $x = L$ at the initial time $t = 0$ by a moving rigid block of mass M_b with initial velocity V_b. The resulting motion of the rod is assumed to be one-dimensional with longitudinal displacement $u(x,t)$ as shown in Fig. 1.

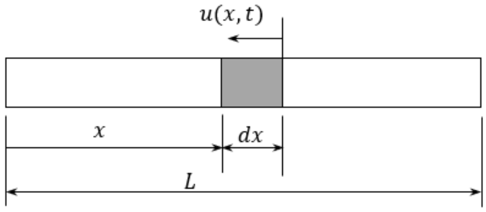

Figure 1. Displacement $u(x,t)$ of the rod at position x.

The equation of motion of the longitudinal wave in the rod is

$$\frac{\partial^2 u(x,t)}{\partial t^2} = {c_o}^2 \frac{\partial^2 u(x,t)}{\partial x^2}, \qquad 0 \leq x \leq L \tag{1}$$

where c_o is the longitudinal wave propagation velocity,

$$c_o = \sqrt{E/\rho} \tag{2}$$

Manuscript received May 11, 2021; revised August 14, 2021.

doi: 10.18178/ijmerr.10.11.626-632

The normal strain $\varepsilon(x,t)$ and stress $\sigma(x,t)$ in the rod are given by:

$$\varepsilon(x,t) = \frac{\partial u(x,t)}{\partial x} \tag{3}$$

$$\sigma(x,t) = E\frac{\partial u(x,t)}{\partial x} \tag{4}$$

The contact force equals the stress at the contact end times the cross-section area of the rod, i.e.

$$F = EA\frac{\partial u(L,t)}{\partial x} \tag{5}$$

According to Saint-Venant's contact theory, at the instant of the impact, the velocity of the contact end $(x = L)$ of the stationary rod immediately equal to the velocity of the striking mass (V_b). The rigid mass remains in contact with the rod as long as the contact force is compressive. We define the contact period t_c as the time during which the contact force between the rigid mass and the rod tip remains compressive. After that time, the mass is no longer in contact with the rod, and the rod performs free vibration, and its motion is controlled by equation (1). The boundary conditions during the contact and after the cease of impact are:

At $x = 0$ for $t > 0$

$$\begin{cases} u(0,t) = 0 & (Fixed) \\ \dfrac{\partial u(0,t)}{\partial x} = 0 & (free) \\ AE\dfrac{\partial u(0,t)}{\partial x} = ku(0,t) & (elastic) \end{cases} \tag{6}$$

And at $x = L$:

- For $0 < t \le t_c$

$$EA\,\frac{\partial u(L,t)}{\partial x} = -M_b\,\frac{\partial^2 u(L,t)}{\partial t^2} \tag{7}$$

- For $t > t_c$

$$EA\,\frac{\partial u(L,t)}{\partial x} = 0 \tag{8}$$

And the initial conditions at $t = 0$ are

$$u(x,0) = 0 \qquad for \quad 0 \le x \le L \tag{9}$$

$$\frac{\partial u(x,0)}{\partial t} = 0 \qquad for \quad 0 \le x < L \tag{10}$$

$$\frac{\partial u(x,0)}{\partial t} = -V_b \qquad at \quad x = L \tag{11}$$

III. FINITE ELEMENT MODELLING AND ALGORITHMS

The finite element formulation for the pre-mentioned wave equation is derived by assuming that

$$u(x,t) = [N]\{U(t)\} \tag{12}$$

where u is the displacement vector, [N] is the matrix of shape functions, and U is the vector of nodal displacement that is assumed to be a function of time t.

Lagrange's equation has been used to obtain the equation of motion which have the following form

$$[M]\{\ddot{U}\} + [K]\{U\} = \{f(t)\} \tag{13}$$

where $[M]$ and $[K]$ are the global mass and stiffness matrices and $\{f(t)\}$ is the global force vector, and $\{U\}$, $\{\dot{U}\}$, $\{\ddot{U}\}$ are the displacement, velocity, and acceleration vectors.

The rod is divided into n linear elements which give $N = \mathrm{n} + 1$ global nodes and the Newmark time integration method is used in the simulation. The initial conditions are:

$$U_i = 0 \qquad for \quad i = 1,2,\dots,N \tag{14}$$

$$\dot{U}_i = 0 \qquad for \quad i = 1,2,\dots,N-1 \tag{15}$$

$$\dot{U}_N = V_b \tag{16}$$

The boundary conditions at the contact end are:

$$F_N = -M_b\ddot{U} \qquad for \quad 0 < t < t_c \tag{17}$$

$$F_N = 0 \qquad for \quad t > t_c \tag{18}$$

where the F_N is the force at the contact end. The displacement, velocity, and acceleration of the block are the same as those of the bar tip as long as the F_N is negative.

During the simulation, we monitor the sign of the F_N and whenever it becomes positive, it remarks the separation of the striking mass from the rod and they lose contact. Hence, we switch to the condition $F_N = 0$ and the rod and the mass are treated separately.

Slight numerical damping is introduced in the Newmark time integration method [23], to reduce the oscillation in the solution, by assuming $\delta = 0.52$ and $\alpha = 0.25 \times (0.5 + \delta)^2$ for the Newmark's integral parameters.

IV. NUMERICAL SIMULATION

To investigate the influence of the support condition of the rod on the contact force, the contact duration, and the stress wave propagation, numerical simulations are presented. An aluminum rod and a striking mass are considered. The material and geometric properties are shown in Table I. It can be noticed that the striking mass has the same mass as the rod ($M_b = \rho AL$).

TABLE I. MATERIAL AND GEOMETRIC PROPERTIES OF THE ROD AND THE STRIKING MASS.

Rod				Rigid mass	
$L(m)$	$A(m^2)$	ρ (kg/m^3)	E (GPa)	M_b (kg)	V_b(m/s)
2.5	0.00025	2700	70	1.6875	−1

We define the dimensionless time τ to show the stress wave propagation and its reflection from the constraint end through the rod during the contact time where

$$\tau = tc_o/L \tag{19}$$

A. Longitudinal Impact for a Fixed-free Rod

Here we consider the longitudinal vibration and stress of the fixed-free rod which is fixed at $x = 0$ and impacted by the moving rigid mass at the free end $x = L$ as shown in Fig. 2.

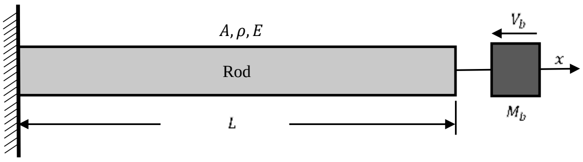

Figure 2. Longitudinal impact of a mass on a fixed-free rod.

The contact force, displacement, and velocity at the impacted end of the rod are shown in Figs. 3-6. The rod displacement is continuous, but both contact force and velocity at the contact end exhibit discontinuities at intervals of 2τ, which correspond to the arrival of the reflection wave from the end of the rod. The black circles on the curves indicate the termination of contact. After the contact time (t_c), the striking mass moves in the positive x-axis with a constant velocity that is the rebound velocity. For the end of the rod at $x = L$, the contact force ceases, i.e., $F_N = 0$, and the simulation presents the free vibration of that end.

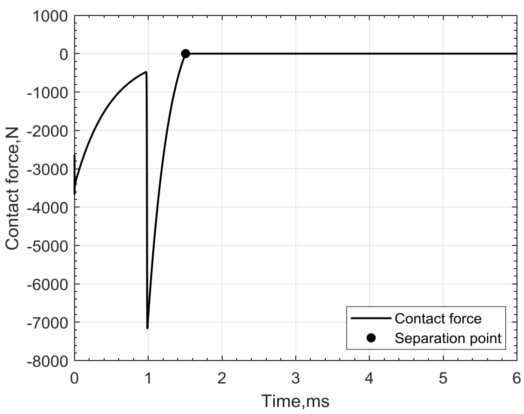

Figure 3. The contact force between the fixed-free rod and the striking mass.

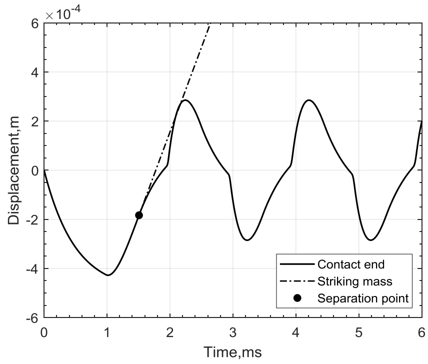

Figure 4. Displacements of contact end and striking mass of the fixed-free rod.

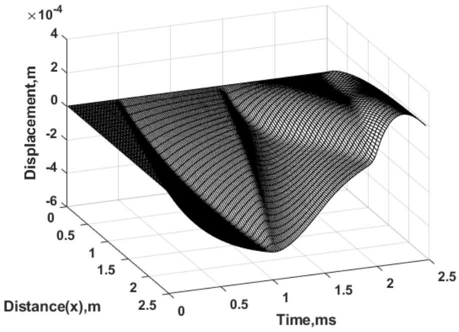

Figure 5. Displacements of the fixed-free rod.

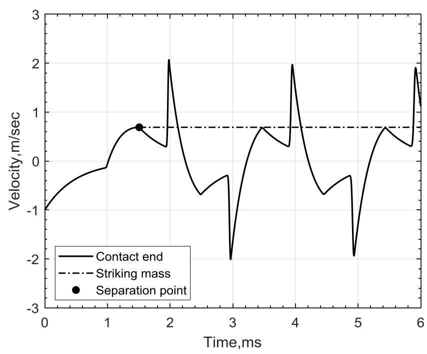

Figure 6. Velocities of contact end and striking mass of the fixed-free rod.

The analytical solution given in [1] predicts the contact time, rebound displacement of contact end, rebound velocity of contact end, and maximum contact force for the longitudinal impact of the fixed-free rod. Both the analytical results and the corresponding results of the current finite element simulation are given in Table II.

TABLE II. COMPARISON BETWEEN THE ANALYTICAL AND THE FINITE ELEMENT RESULTS (FIXED – FREE ROD)

Item	Analytical Results [1]	Proposed Finite Element Results
Contact time	0.001506 $sec.$	0.001506 $sec.$
Maximum contact force	$-7.335 \times 10^3\ N$	$-7.1575 \times 10^3\ N$
Rebound displacement	$-0.1842\ mm$	$-0.18413\ \mathrm{m}m$
Rebound velocity	0.6876 m/sec	0.6879 m/sec

As shown in Figs. 7-10, there is no deformation in the undisturbed region until the stress wave arrives. The compressive stress wave, which travels through the rod, is reflected from the fixed end as a compressive wave at time $\tau = 1$ or $t = 0.48902ms$. During the contact period, the contact tip works as a fixed end, and the compressive wave is reflected from that end as a compressive wave again at time $\tau = 2$. So, the whole rod is under compression during the contact period. The arrival of the reflected compression wave to the contact end raises the stress at the contact end, and accordingly, the contact force reaches its maximum value.

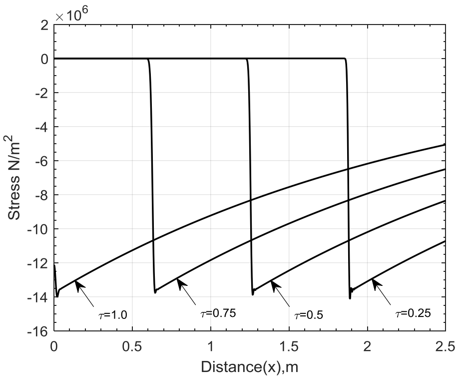

Figure 7. Stress wave propagation in the fixed-free rod from the contact end to the fixed end.

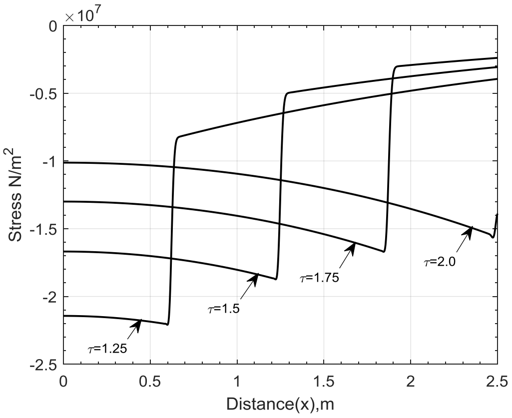

Figure 8. Propagation of the reflected wave from the fixed end to the contact end of the fixed-free rod.

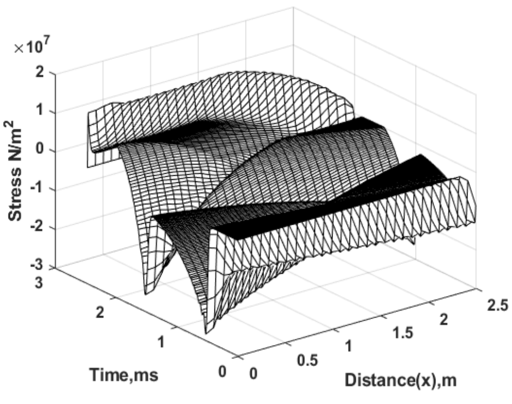

Figure 9. The stress of the fixed-free rod.

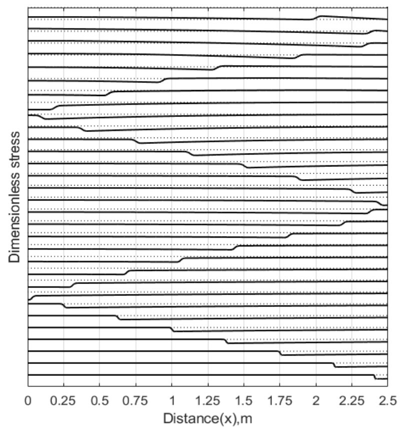

Figure 10. Propagation of the stress wave in the fixed-free rod. Stress distributions are shown every 0.1500 dimensionless time.

B. Longitudinal Impact for a Free- free Rod

The free-free rod and the striking mass are shown in Fig. 11. The contact force, displacement, and velocity at the impacted end of the rod are shown in Figs. 12-15. The displacement and velocity for both the free end of the rod and the striking mass are presented in Figs. 13 and 15. The black circles on the curves indicate the termination of contact. The rod displacement is continuous, but both contact force and velocities of both ends of the rod exhibit discontinuities at intervals of 2τ, which correspond to the arrival of the reflection wave from the end of the rod.

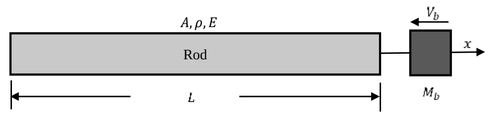

Figure 11. Longitudinal impact of a mass on a free-free rod.

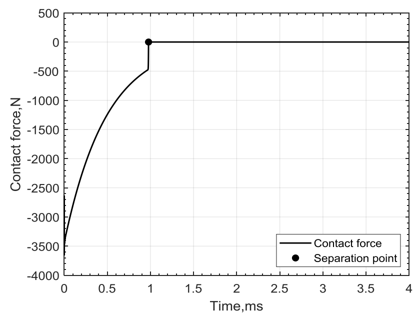

Figure 12. The contact force between the free-free rod and the striking mass.

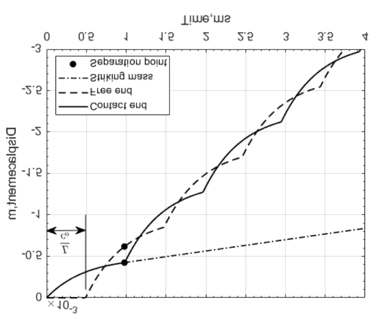

Figure 13. Displacements of contact end, striking mass, and the free end of the free-free rod.

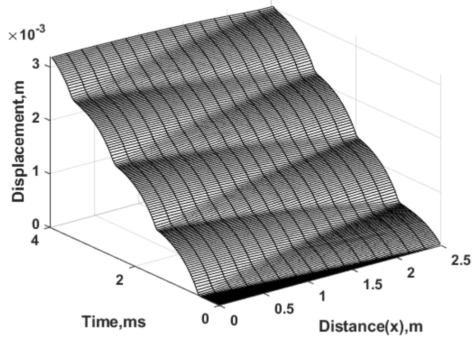

Figure 14. The magnitude of displacement of the free-free rod.

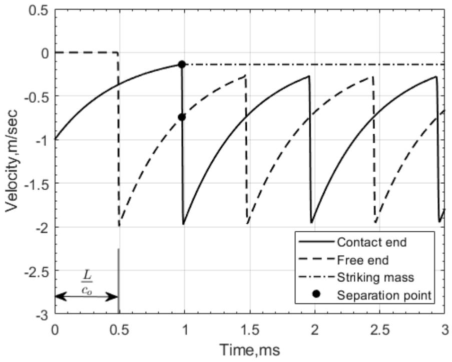

Figure 15. Velocities of contact end, striking mass, and the free end of the free-free rod.

The contact time, rebound displacement of contact end, rebound velocity of contact end, and maximum contact force for the impact of the free-free rod given in Table III.

TABLE III. THE FINITE ELEMENT RESULTS (FREE-FREE ROD)

Item	Proposed Finite Element Results
Contact time	0.97805 ms.
Maximum contact force	$-3.6522 \times 10^3\ N$
Rebound displacement	$-0.42422\ mm$
Rebound velocity	$-0.1370\ m/sec.$

As illustrated in Figs. 16-18, the reflected stress wave is opposite to the incident stress wave, thus, the compression wave reflects as a tension wave and vice versa. This stress reversal is a characteristic of the free end. However, at the contact tip, when the tension wave reaches this tip, it cancels the stress to zero, and contact is terminated at dimensionless time $\tau = 2$.

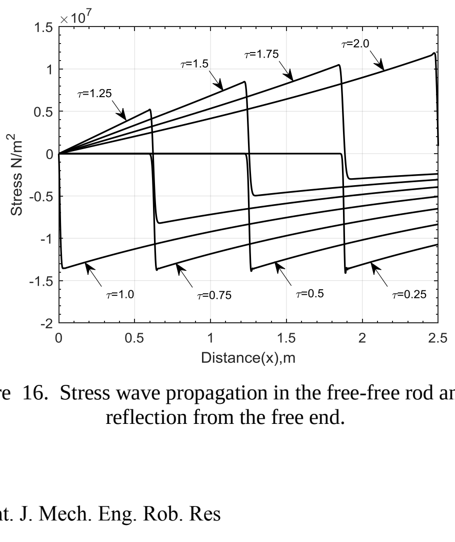

Figure 16. Stress wave propagation in the free-free rod and its reflection from the free end.

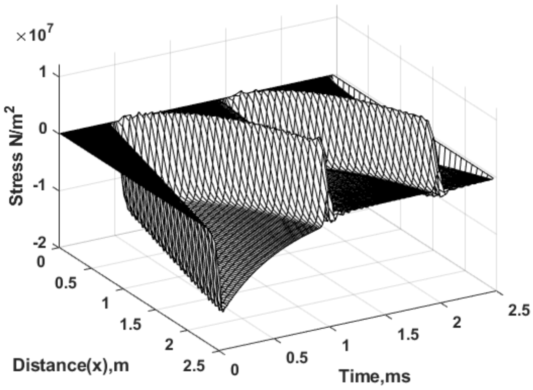

Figure 17. The stress of the free-free rod.

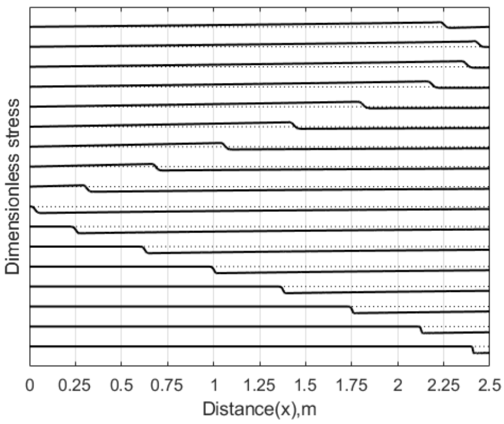

Figure 18. Propagation of the stress wave in the free-free rod. Stress distributions are shown every 0.1500 dimensionless time.

C. Longitudinal Impact for a Rod Attached to a Spring

Here we consider the longitudinal impact between the rigid mass and the aluminum rod which is attached to a spring whose stiffness is k, as shown in Fig. 19. The contact force, displacement, and velocity at the impacted end of the rod are shown in Figs. 20-22. The black circles on the curves indicate the termination of contact. The rod displacement is continuous, but both contact force and velocities of both ends of the rod exhibit discontinuities at intervals of $2L/c_o$, which correspond to the arrival of the reflection wave from the end of the rod.

It should be noted that when $0 \le \tau < 1$, the contact force is independent of the constraint of the left end $x = 0$ and the results are the same whatever the boundary condition of the end is. So, when $0 \le \tau < 1$, the constraint of the left end, i.e., $0 \le k \le \infty$ has not any effects on the impact loads.

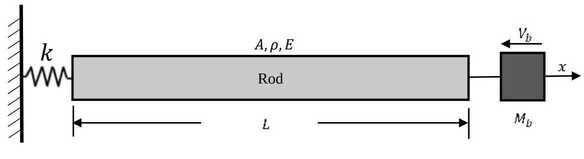

Figure 19. Longitudinal impact of a mass on the rod with spring.

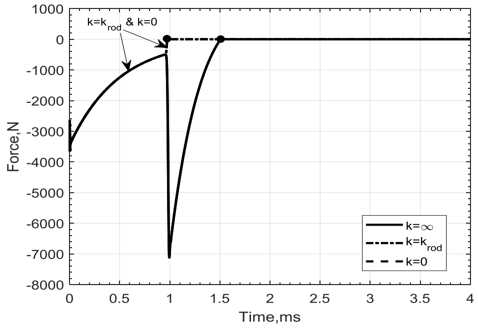

Figure 20. The contact force between the rod tip and the striking mass.

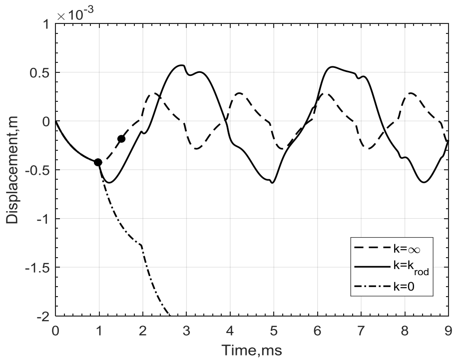

Figure 21. Displacement of the contact end of the rod attached to a spring.

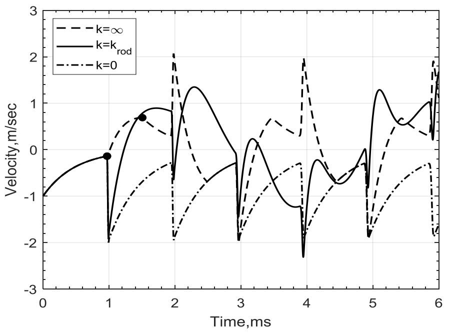

Figure 22. The velocity of the contact end of the rod attached to a spring.

The wave propagation in the rod when $k = k_{rod}$ is shown in Fig. 23. The reflected wave is something between the reflected wave for the fixed end and the reflected wave for the free end. The finite element results agree with those by the method of mode superposition very well [22].

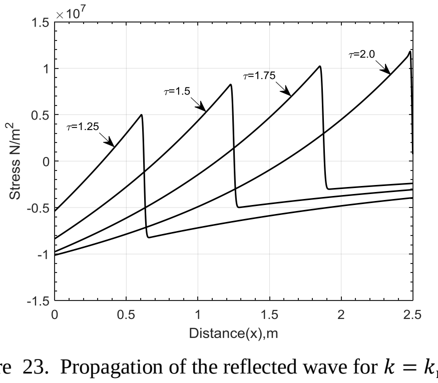

Figure 23. Propagation of the reflected wave for $k = k_{\mathrm{rod}}$.

V. Conclusions

Based on Saint-Venant's contact theory, the dynamic response and stress wave propagation for the longitudinal impact between a rigid mass and a uniform elastic rod with rigid, free, and deformable support conditions have been analyzed. A finite element formulation combined with the Newmark time integration method has been utilized to investigate the effect of the boundary conditions on the stress propagation, contact forces, displacements, and velocities. The displacement and velocity of the striking mass have been illustrated also. The presented visualization of the stress wave propagation enhances the understanding of the considered physical phenomenon. The results confirm that the developed finite element analysis provides a convenient, accurate, and applicable means to investigate this complex incident.

Conflict of Interest

The authors declare no conflict of interest.

Author Contributions

Prof. Elkaranshawy and Dr. Elabsy provided background information and the necessary resources for the research. Mr. Etiwa conducted the research and wrote the paper. Prof. Elkaranshawy and Mr. Etiwa discussed and analyzed the results. All authors had approved the final version.

References

[1] W. Goldsmith, *Impact: The Theory and Physical Behavior of Colliding Solids*, 1st ed. London: Edward Arnold, 1960, ch.3, pp. 22-56.

[2] K. F. Graff, *Wave Motion in Elastic Solids*. Oxford University Press., 1975, ch.2, pp. 75-110.

[3] S. Timoshenko, *Vibration Problems in Engineering*, 2nd ed. D. van Nostrand Company Inc., New York, USA., 1937, ch.VI, pp. 397-405.

[4] A. E. H. Love, M. A., D. Sc., and F. R. S., *A Treatise on The Mathematical Theory of Elasticity*, 4th ed. New York Dover Publications, 1944, ch.XX, pp. 397-405.

[5] W. Johnson, *Impact Strength of Materials*, 1st. Edward Arnold, 1972, ch.1, pp. 1-62.

[6] M. M. Al-Mousawi, "On experimental studies of longitudinal and flexural wave propagations: An annotated bibliography," *Appl. Mech. Rev*., vol. 39, no. 6, pp. 853–865, 1986.

[7] Elkaranshawy Hesham A. and N. S. Bajaba., "A finite element simulation of longitudinal impact waves in elastic rods," in *Materials with Complex Behaviour II*, Springer Heidelberg Dordrecht London New York 2012, ch1, pp. 13-27.

[8] B. A. Gama, S. L. Lopatnikov, and J. W. Gillespie Jr., "Hopkinson bar experimental technique: A critical review," *Appl. Mech. Rev*, vol. 57, no. 4, pp. 223–250, 2004.

[9] R. B. Malla, M. Asce, and T. G. Gionet, "Dynamic response of a pressurized frame-membrane lunar structure with regolith cover subjected to impact load," *J. Aerosp. Eng*., vol. 26, no. 4, pp. 855–874, 2013.

[10] R. B. Malla and L. J. Vila, "Dynamic impact force in an axial member with coupled effects of structural vibration and various support conditions," *Eng. Struct*., vol. 144, pp. 210–224, 2017.

[11] H. Ram ́ırez and C. Rubio-Gonzalez, "Finite-element simulation of wave propagation and dispersion in Hopkinson bar test," *Mater. Des*., vol. 27, no. 1, pp. 36–44, 2006.

[12] X. Li, T. Zhou, and D. Li, "Dynamic strength and fracturing behavior of single-flawed prismatic marble specimens under impact loading with a Split-Hopkinson pressure bar," *Rock Mech. Rock Eng*., vol. 50, no. 1, pp. 29–44, 2017.

[13] M. Hassan and K. Wille, "Experimental impact analysis on ultra-high performance concrete (UHPC) for achieving stress equilibrium (SE) and constant strain rate (CSR) in Split Hopkinson pressure bar (SHPB) using pulse shaping technique," *Constr. Build. Mater*., vol. 144, pp. 747–757, 2017.
[14] T. C. Togami, W. E. Baker, and M. J. Forrestal, "A split Hopkinson bar technique to evaluate the performance of accelerometers," *J. Appl. Mech.*, vol. 63, pp. 353–356, 1996.
[15] Z. Yang, Q. Wang, H. Du, J. Fan, and J. Liang, "Dynamic characterization method of accelerometers based on the Hopkinson bar calibration system," *Sensors and Actuators*, vol. 293, pp. 21–28, 2019.
[16] H. A. Elkaranshawy, "Stress waves in a damaged rod subjected to longitudinal impact," *Int. J. Mech. Eng. Robot. Res.*, vol. 8, no. 3, pp. 488–493, 2019.
[17] H. A. Elkaranshawy and N. S. Bajaba, "Damage detection in an elastic rod using finite element simulation to longitudinal impact waves," in *Proc. 15th International Congress on Sound and Vibration*, 2008.
[18] H. A. Elkaranshawy and N. S. Bajaba, "A finite element simulation to longitudinal impact waves in elastic rods," *Int. J. Appl. Eng. Res.*, vol. 3, no. 6, pp. 847–860, 2008.
[19] S. A. Ragab and H. E. Fayed, *Introduction to Finite Element Analysis for Engineers*, 1st ed. CRC Press Taylor & Francis Group Boca Raton London New York CRC, 2018, ch.6, pp. 468-476.
[20] Y. Shen and X. Yin, "Dynamic substructure analysis of stress waves generated by impacts on non-uniform rod structures," *Mech. Mach. Theory*, vol. 74, pp. 154–172, 2014.
[21] Y. Shen and X. Yin, "Analysis of geometric dispersion effect of impact-induced transient waves in composite rod using dynamic substructure method," *Appl. Math. Model.*, vol. 40, no. 3, pp. 1972–1988, 2016.
[22] X. YuFeng, and Z, DeChao, "Analytical solutions of impact problems of rod structures with springs," *Computer Methods in Applied Mechanics and Engineering*, vol.160, no. 3-4, pp. 315-323, 1998.
[23] K.-J. Bathe, *Finite Element Procedures*, 2nd ed. 2015.

Ragab M. Etiwa was born in Beheira, Egypt, in 1992. He received his B.Sc. (distinction with a degree of honor) in mechanical power engineering from Alexandria University, Egypt, in 2015. He is currently pursuing his M.Sc. degree in engineering mathematics in the Department of Engineering Mathematics and Physics, Faculty of Engineering, Alexandria University, Egypt. He worked as a Project Engineer in the project of Egyptian Refining Company (ERC) in Cairo, Egypt, and Burullus Power Plant 4800 MW (the project of Middle Delta Electricity Production Company), Egypt. He has occupied a teaching/research position in the Department of Engineering Mathematics and Physics, Faculty of Engineering, Alexandria university since September 2016.

Hanaa M. Elabsy was born in Kafr El-Sheikh, Egypt in 1959. She received her BSc degree (distinction with a degree of honor) in Mechanical Engineering, MSc and Ph.D. degrees in Engineering Mathematics from Alexandria University, Egypt in 1997. She was a visiting scholar at the University of Illinois Chicago between 1995 and 1997. She has served as an assistant professor and teaching faculty in the Department of Physics and Engineering Mathematics at Alexandria University since 1997. Her research interests include mechanical vibration and multibody dynamics.

Hesham A. Elkaranshawy was born in Alexandria, Egypt in 1961. He received his BSc degree (distinction with a degree of honor) in mechanical power engineering and MSc degree in Engineering Mathematics from Alexandria University, Alexandria, Egypt, in 1983 and 1988 respectively. He received his Ph.D. degree in Mechanical Engineering from McMaster University, Hamilton, Ontario, Canada, in 1995. During 1995-1996 he joined CAE Electronics, Montreal, Canada, as a FINITE ELEMENT SPECIALIST where he was involved in the design of the company's flight simulators and their role in the world space station project. He became an ASSISTANT PROFESSOR at the Department of Engineering Mathematics and Physics, Engineering Mechanics Division, Alexandria University in 1996. In 1998 he established *Dynamic* Engineering Consultants, Giza, Egypt. In 2001, He became an ASSISTANT PROFESSOR at the Department of Mechanical Engineering, Yanbu Industrial College, Royal Commission for Jubail and Yanbu, Saudi Arabia. Since 2010 he went back to Alexandria University and is now a PROFESSOR of Engineering Mathematics and Engineering Mechanics at the Department of Engineering Mathematics and Physics.
Prof. Elkaranshawy was a board member of the Egyptian Syndicate for Engineers in Behera province. Many of his scientific papers are published in international journals. His research interests include multibody dynamics, robot dynamics, contact-impact dynamics, finite element modeling, mechanical vibrations, wave propagation, fault detection, nonlinear systems, mathematical biology, and ordinary differential equations.